processes

MDPI

Article

Effect of Calcination Temperature on the Structural and Electrochemical Behaviour of Li-Based Cathode for Intermediate-Temperature SOFC Application

Sumarni Mansur, Nurul Akidah Baharuddin *, Wan Nor Anasuhah Wan Yusoff, Azreen Junaida Abd Aziz and Mahendra Rao Somalu

Solid Oxide Fuel Cell Group, Fuel Cell Institute, Universiti Kebangsaan Malaysia, UKM, Bangi 43600, Selangor, Malaysia

* Correspondence: akidah@ukm.edu.my

Abstract: A new strategy to reduce the operating temperature of the solid oxide fuel cell (SOFC) is needed to foster the progress of developing high-performance and stable SOFC as a solution to the thermal stress and degradation of the cell components induced by high-temperature SOFC. The use of lithium (Li) as a cathode can increase the cell's efficiency, as it allows for faster ion transport and a higher reaction rate. This study presents an attractive approach to using a Li-based cathode by combining Li with cobalt (Co) to form $LiCo_{0.6}Sr_{0.4}O_2$ (LCSO). In this work, a precursor consisting of Li, Co, and strontium (Sr) was prepared via the glycine-nitrate combustion method. The precursor was calcined at two different calcination temperatures (800 and 900 °C) prior to ink formulation and symmetrical cell fabrication in order to study the effect of calcination temperature on the structural and electrochemical behaviour of a Li-based cathode. The precursor LCSO powder was characterised using X-ray crystallography (XRD) to determine the crystal structure and composition of the developed LCSO. The electrochemical performance of the fabricated symmetrical cell was tested using electrochemical impedance spectroscopy (EIS) to obtain the cell's resistance information, which is related to the cell's ionic and electronic conductivity. SDC electrolyte with LCSO calcined at 800 °C has a higher crystallinity percentage and a more porous structure compared to LCSO calcined at 900 °C. The porous structure enhanced the electrochemical performance of the cell, where the symmetrical cell has the highest conductivity (0.038 Scm^{-1}) with the lowest activation energy (0.43 eV). The symmetrical cell was also able to achieve 2.89 Ω cm^2 of area-specific resistance (ASR) at 800 °C of operating temperature. In conclusion, the SDC electrolyte with LCSO calcined at 800 °C is the promising cathode material for SOFC applications. The result of this study can benefit the SOFC field of research, especially in the development of intermediate temperature-SOFC.

Keywords: solid oxide fuel cell; lithiated cathode materials; symmetrical cell; microstructure; electrochemical performance

check for updates

Citation: Mansur, S.; Baharuddin, N.A.; Wan Yusoff, W.N.A.; Abd Aziz, A.J.; Somalu, M.R. Effect of Calcination Temperature on the Structural and Electrochemical Behaviour of Li-Based Cathode for Intermediate-Temperature SOFC Application. *Processes* **2023**, *11*, 2139. https://doi.org/10.3390/pr11072139

Academic Editor: Antonio Bertei

Received: 24 May 2023
Revised: 21 June 2023
Accepted: 21 June 2023
Published: 18 July 2023

Copyright: © 2023 by the authors. Licensee MDPI, Basel, Switzerland. This article is an open access article distributed under the terms and conditions of the Creative Commons Attribution (CC BY) license (https://creativecommons.org/licenses/by/4.0/).

1. Introduction

Solid oxide fuel cells (SOFCs) are promising energy conversion devices that can directly convert the chemical energy of fuels into electrical energy. Fundamentally, SOFCs use the movement of electrons and ions to generate electricity. It started when the fuel such as natural gas, biomethane, or hydrogen (H_2) and oxygen (O_2) gas passed through the core of the SOFC. The molecules of H_2 and O_2 gases were split into their respective elements and then reacted with one another, converting the fuel to electricity and heat [1]. The normal SOFC's operating temperature is between 600 °C and 1000 °C, which is the highest operating temperature among other fuel cells. The main reason for the high operating temperature is to reach high ion conductivity in the electrolyte [2]. At high temperatures, the solid oxide electrolyte allows for high ionic conductivity, enabling the

efficient electrochemical reaction between the fuel and the oxidant [3]. However, the high operating temperature of SOFCs has various consequences on the performance, durability, and stability of the SOFCs system. In the long term, the high temperature can cause the SOFC system to degrade due to thermal stress, chemical degradation, and mechanical failure [4–6]. These also affect the cooling and insulation costs for the system, which can limit the scalability and commercialisation of SOFCs. Many efforts have been made to reduce the operating temperature while maintaining the performance of the SOFCs. SOFCs that operate at temperatures between 500 °C and 700 °C can be defined as intermediate-temperature SOFCs (IT-SOFCs) [7–9]. IT SOFCs offer several advantages, including faster start-up, lower material degradation, and reduced operating costs. However, reducing the operating temperature would significantly reduce the electrochemical performance of the cell due to reduced ionic conductivity of the electrolyte and poor catalytic activity of the electrodes [10]. Thus, comprehensive strategies need to be employed, such as material optimisation, doping technique improvement, electrode design development, fuel processing development, system integration, and others.

One main approach to lowering the operating temperature of SOFCs is through the use of cathode materials that promote electrochemical activity at lower temperatures [1,10,11]. In this context, Li-based cathodes have shown great potential for IT-SOFC applications due to their high electrochemical activity and thermal stability. The structural and electrochemical properties of Li-based cathodes are affected by various processing parameters, including the calcination temperature. The calcination temperature plays a crucial role in determining the crystal structure, phase purity, and morphology of the cathode material. It can also affect the electrochemical performance of the cathode by altering the surface area, porosity, and particle size distribution. A higher calcination temperature can lead to a more well-defined crystal structure, resulting in improved electrochemical activity and ionic conductivity at lower temperatures [12]. While a lower calcination temperature can result in a more porous structure, which can improve the accessibility of reactants to the cathode-electrolyte interface and promote the oxygen reduction reaction (ORR) at lower temperatures [13–15]. Therefore, the optimisation of the calcination temperature is critical to achieving high-performance Li-based cathodes for IT-SOFC applications.

Lithium cobalt strontium oxide ($LiCo_{0.6}Sr_{0.4}O_2$ or LCSO) is a complex cathode material consisting of lithium (Li), cobalt (Co), strontium (Sr), and oxygen (O) atoms. Li is an essential component of LCSO cathode material as it contributes to its electronic conductivity and promotes the ORR at the cathode-electrolyte interface. Li ions are mobile in the cathode material, allowing them to migrate to the surface and participate in the ORR process [16]. This results in high electrochemical activity and improved overall performance of the LCSO cathode. Co is another critical component of the LCSO cathode material. Co ions act as the active sites for the ORR process and help to improve the electronic conductivity of the cathode material [17]. Additionally, Co ions contribute to the crystal structure of LCSO and help to stabilize the material under high-temperature operating conditions [18]. Sr is also an important component of the LCSO cathode material as it contributes to its ionic conductivity and thermal stability. The addition of Sr to LCSO helps to enhance the material's electronic conductivity, which is essential for efficient electron transfer during the ORR process [19]. Additionally, Sr helps to stabilize the crystal structure of the cathode material and improve its thermal compatibility with the electrolyte [19]. This reduces the risk of delamination and cracking, which can occur when the cathode and electrolyte have different thermal expansion coefficients. Each of these elements plays a critical role in determining the electrochemical properties and performance of the LCSO cathode material.

Choosing a suitable electrolyte is crucial for the performance and efficiency of SOFCs. The electrolyte serves as the pathway for the movement of oxygen ions from the cathode to the anode. It is essential to select an electrolyte material with high ionic conductivity to facilitate efficient ion transport [20]. A suitable electrolyte with high ionic conductivity minimizes the resistance encountered by the ions during the ion's migration, reducing the overall electrical losses in the cell [8,15,21]. Both Yttria-stabilised Zirconia (YSZ) and

Samarium-doped Ceria (SDC) are commonly used electrolyte materials in various electrochemical devices. YSZ is a solid solution of zirconium dioxide ($ZrCO_2$) and yttrium oxide (Y_2O_3) [22]. The yttrium ions (Y^{3+}) are introduced into the zirconium lattice to stabilize its structure at high temperatures and enhance oxygen ion conductivity [8]. The presence of yttrium ions creates oxygen vacancies within the crystal lattice, which allows for the migration of oxygen ions through the material [21,23]. SDC is a solid electrolyte material that exhibits high ionic conductivity at intermediate temperatures. In SDC, samarium (Sm) ions are doped into a cerium oxide (CeO_2) lattice, resulting in the formation of a mixed ionic-electronic conductor [24]. The presence of samarium dopant enables the material to exhibit enhanced oxygen ion conductivity, making it a suitable electrolyte for fuel cells and other applications that involve oxygen transport [25].

The objective of this study is to investigate the effect of the calcination temperature on the structural and electrochemical behaviour of LCSO cathodes for IT-SOFC applications. In this study, LCSO cathodes are synthesised at different calcination temperatures, and their crystal structure, phase purity, morphology, and electrochemical performance are characterised accordingly. The results of this study will provide insights into the optimal calcination temperature for LCSO cathodes, and the impact of calcination temperature on the structural and electrochemical properties of the cathode material. The findings of this study will contribute to the design and optimisation of high-performance Li-based cathodes for IT-SOFC applications.

2. Experimental

2.1. Materials

Lithium nitrate ($LiNO_3$), strontium nitrate ($Sr(NO_3)_2$ > 99% ACS Reagent), and glycine ($C_2H_5NO_2$) were purchased from Sigma Aldrich (St-Louis, MO, USA, St-Louis, USA and Burlington, NJ, USA, respectively). Cobalt nitrate hexahydrate ($Co(NO_3)_2{\cdot}6H_2O$, 98% Reagent Grade) was obtained from Merck Chemicals, Billerica, MA, USA. Yttria-stabilised zirconia (YSZ, 8 mol%, TZ-8Y) and Samarium doped ceria, $Ce_{0.8}Sm_{0.2}O_{1.9}$ (SDC) were purchased from Tosoh, Yamaguchi, Japan, and Sigma-Aldrich, St-Louis, MO, USA, respectively. Hypermer KD15 (dispersant) was purchased from Croda (Yorkshire, UK). Meanwhile, anhydrous terpineol solvent and ethyl cellulose N7 grade (binder, 0.25–0.5 wt%) were obtained from Sigma-Aldrich (Billerica, MA, USA) and Sigma-Aldrich (St-Louis, MO, USA), respectively.

2.2. Synthesis and Characterisation of $LiCo_{0.6}Sr_{0.4}O_2$ Cathode Powder

The LCSO was synthesised via the glycine-nitrate combustion (GNC) method, as described in our previous studies by Yusuff et al. and Tahir et al. [26–28]. The flow of the synthesis procedure was illustrated in Figure 1; 0.6 mol of $Co(NO_3)_2{\cdot}6H_2O$ was mixed with 0.4 mol of $Sr(NO_3)_2$ in a beaker filled with 100 mL of deionised water. The mixture was stirred on a magnetic hotplate stirrer for 10 min until all the powders were dissolved homogeneously. Next, 1 mol of $LiNO_3$ was added to the solution and stirred for another 30 min; 2 mol of $C_2H_5NO_2$ was added to the nitrate solution as a combustion agent (fuel). The precursor solution was left to stir for 18 h at room temperature prior to being heated (250–300 °C) to initiate the combustion. Ash composed of the oxides produced from the self-sustaining combustion was dried in a drying oven (Ecocell, Vantaa, Finland) for approximately 12 h at 100 °C to remove excess water. The powder obtained was calcined at 800 °C and 900 °C at a heating and cooling rate of 10 °C/min in a high-temperature compact muffle furnace (Berkeley Scientific, Berkeley, CA, USA) for 5 h. Figure 2a shows the physical colour of the powder before and after calcination. The calcined powder was ground and sieved using a 212 µm laboratory test sieve (Impact-test, London, UK). The crystallisation and chemical composition of the synthesised powders were analysed using X-ray diffraction (XRD, Bruker AXS D8 Advance, Germany). The analysis was tested for 2θ range from 20° to 70° at 40 kV and 40 mA generator with a divergence slit of 0.3°. Inductively coupled plasma mass spectrometry (ICP-MS) was used to determine the

chemical composition of the synthesised LCSO powder; 200 ppm of LCSO stock solution was prepared by diluting 10 mg of LCSO powder into 10 mL of nitric acid and 40 mL of deionised water; 1 ppb from the stock solution was employed in a NexION 2000 ICP-MS (PerkinElmer, Shelton, CT, USA), and PerkinElmer Syngistix software V 2.5 was used to analyse the data. The XRD and ICP-MS analysis was done at Center of Research and Instrumentation Management in Universiti Kebangsaan Malaysia.

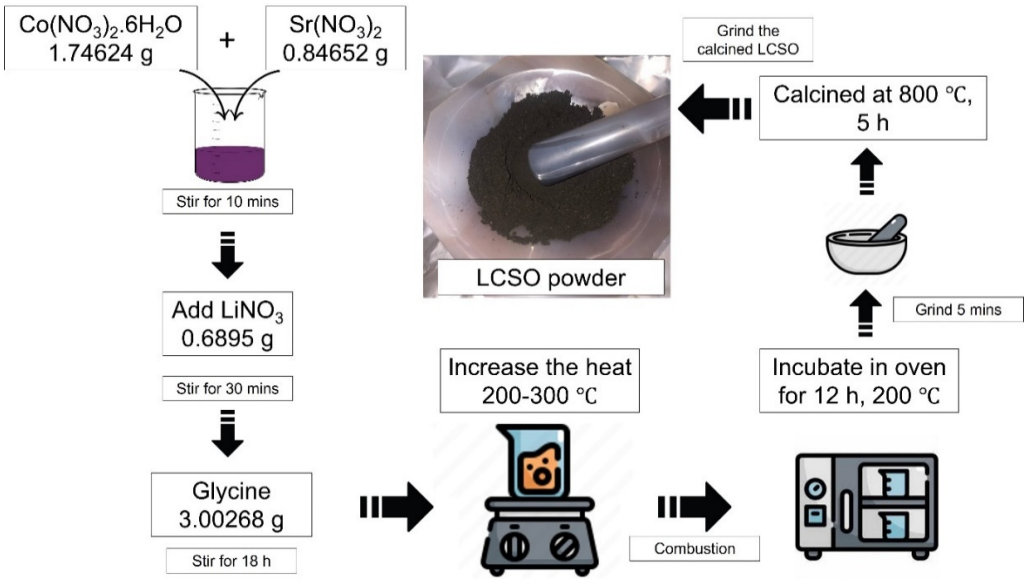


Figure 1. Schematic diagram of LCSO synthesis process via glycine-nitrate process.

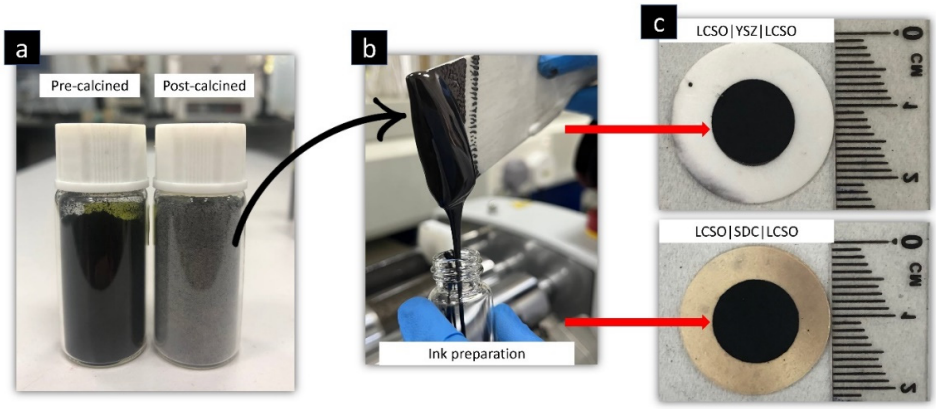


Figure 2. (**a**) LCSO powder before and after calcination (**b**) Collected LCSO ink after milling process (**c**) LCSO cathode film on YSZ and SDC electrolyte button pellets forming symmetrical cell.

2.3. LCSO Ink Preparation

The calcinated LCSO powders were mixed with a dispersant (hypermer KD15) and ball-milled for 10 min at 1500 rpm using a high-energy centrifugal planetary mixer (Kakuhunter, Nojihigashi, Kusatsu City, Shiga, Japan). A vehicle solute was prepared by mixing a binder (ethycellulose) and terpineol solvent using a hotplate stirrer for 1 h at 90 °C. The details of the ink composition are shown in Table 1. The ball-milled mixture was then ground with the prepared vehicle prior to the milling process using a triple-roll mill (EXAKT 80E, Norderstedt, Germany). The gap between the first and second rollers was set to 40 µm and the gap between the second and third rollers to 20 µm, respectively. The milling process was set at a speed of 3.5 rpm and repeated three times. The final ink product was collected at the end of the third roller as shown in Figure 2b.

Table 1. Ink composition for LCSO cathode.

Ink/Slurry Composition	LCSO Cathode (wt%)
Density (g cm^{-3})	6.33
Powder	70.3
Dispersant (Hypermer KD15)	1.4
Binder (Ethylcelulose N7)	1.4
Solvent (Terpineol)	26.9
Vehicles (binder + solvent) viscosity (cP)	19.1194

2.4. Symmetrical Cell Fabrication

An evacuable pellet die of 32 mm and 25 mm (Specac Ltd., London, UK) was used as a mould to form 2.5 g of YSZ and 3 g of SDC into button pellets, respectively, as shown in Figure 2c; 1.5 tonnes of pressure were applied to the die containing the YSZ or SDC powder using a hydraulic press machine (Carver Inc., Wabash, IN, USA). The holding time was set to 30 s. The button pellet was carefully transferred to the high-temperature compact muffle furnace (Berkeley Scientific, Berkeley, CA, USA) and sintered at 1400 °C for 6 h, 5 °C/min.

The sintered pellet was mounted on an in-house screen-printing holder. A mesh was placed on top of the pellet. Next, a squeegee was used to apply prepared LCSO ink on both sides of the YSZ and SDC electrolytes, as shown in Figure 2c. Two layers of the LCSO ink with 1 cm^2 of active site were screen-printed in the centre of the cell to construct LCSO | YSZ | LCSO and LCSO | SDC | LCSO symmetrical cells, respectively. The printed button cell was sintered at 800 °C for 2 h, 10 °C/min.

2.5. Characterisation and Electrochemical Analysis of the Symmetrical Cell

The fabricated symmetrical cell was mounted on the current collector setup as shown in Figure 3. The setup was inserted into the tube furnace and connected to the combined sense and working electrode (S + WR), and the combined reference and counter electrode (R + C) of Autolab PGSTAT302N (Autolab 302, Eco Chemie, The Netherlands). The analysis was tested within the frequency range of 0.01 Hz to 1 MHz in potentiostatic mode at an amplitude voltage of 20 mV and a temperature range of 800 to 500 °C. The impedance spectra were plotted into Nyquist plots to determine the area-specific resistance (ASR) of the cathodes. All the data were analysed using the NOVA 2.0 software. Next, the fabricated symmetrical cells were characterised using field emission scanning electron microscopy (FEI, Quanta 400, Houston, TX, USA).

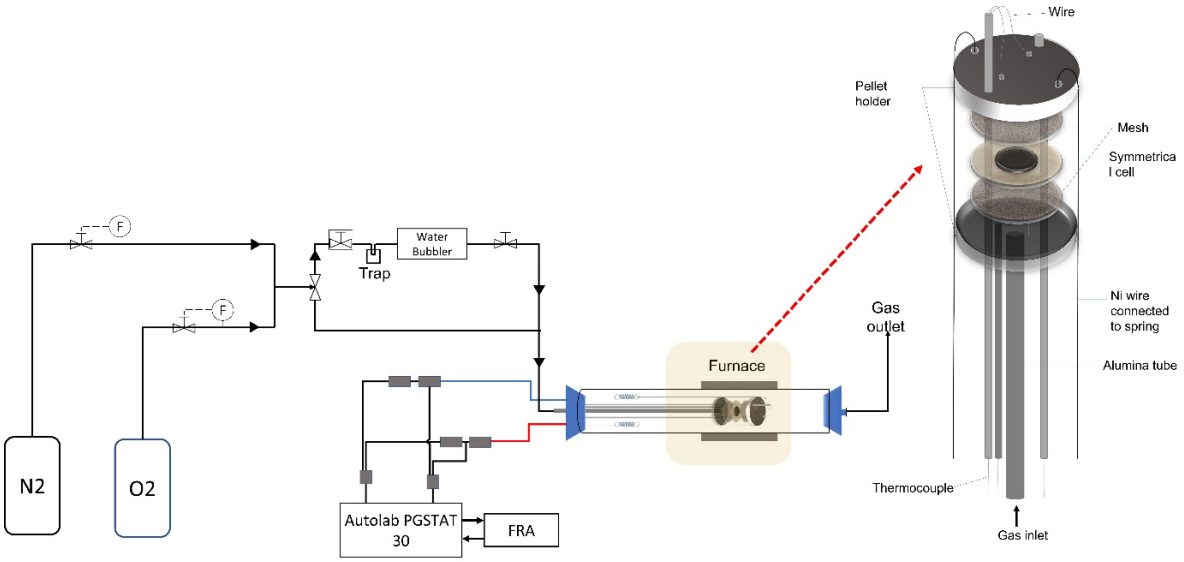


Figure 3. Schematic diagram of electrochemical performance analysis of the symmetrical cell via SOFC symmetrical cell test device.

3. Results and Discussion

3.1. LCSO Physico-Chemical Properties

3.1.1. XRD Analysis

Figure 4 shows the XRD spectrum pattern of the LCSO cathode powder calcined at 800 °C and 900 °C. Both main peaks of the LCSO powders were compared to the Joint Committee on Powder Diffraction Standards (JCPDS) file numbers for lithium cobalt oxide ($LiCoO_2$) (JCPDS file no. 00-050-0653) and strontium cobalt oxide ($SrCoO_3$) (JCPDS file no. 01-074-6262). The most prominent peaks are observed for the (111) and (003) planes, which are characteristic of the strontium cobalt oxide structure. The changes in calcine temperature did not influence the broadening of the lattice. However, the peak intensities of the spectrum significantly change at higher calcination temperatures, as can be seen in the enlargement image of the XRD spectrum in Figure 5. The enlargement of the LCSO peak in Figure 5a showed that the peak intensities at (111) increase with higher calcination temperatures. In Figure 5b, the peaks at (104) and (115) decrease with higher calcination temperatures. This result shows that lattice expansion of strontium cobalt oxide and loss of lithium occurred at 900 °C. Hence, 800 °C should be the optimum temperature for the calcination of the LCSO powder.

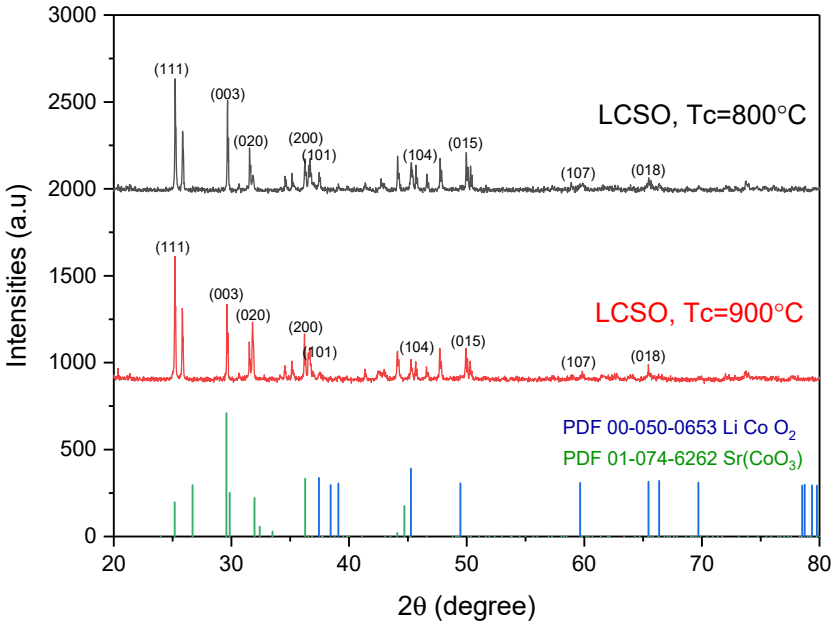


Figure 4. XRD analysis for LCSO powder calcined at different temperature (800 °C and 900 °C).

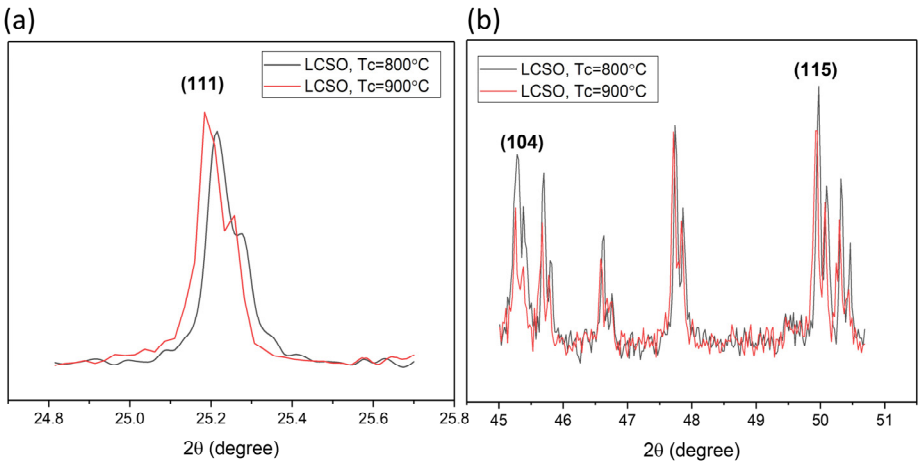


Figure 5. Enlargement of LCSO peak at (**a**) 111 and (**b**) 104 and 115.

Based on the crystallisation analysis in Table 2, LCSO powder calcined at 800 °C shows a higher crystallinity percentage, which is 77.4%, compared to LCSO powder calcined at 900 °C, which has only 70.7%. At 800 °C, the chemical composition analysis shows a higher amount of lithium compared to a 900 °C calcination temperature. Lithium started to disappear while strontium percentage increased at the calcination temperature of 900 °C, which is in coherence with the loss of lithium peak as shown in Figures 4 and 5.

Table 2. Crystallinity percentage and chemical composition of synthesised LCSO powder based on the XRD analysis.

	Tc = 800 °C	**Tc = 900 °C**
% Crystallinity	77.4%	70.7%
% Amorphous	22.6%	29.3%
Li	SQD = 10.342%	SQD = 8.348%
Co	SQD = 64.292%	SQD = 59.321%
Sr	SQD = 17.176%	SQD = 24.134%
Lithium cobalt oxide ($LiCoO_2$)	67.751%	54.666%
Strontium cobalt oxide ($Sr(CoO_3)$)	32.249%	45.314%

Tc: Calcined temperature.

3.1.2. ICPMS Analysis

The chemical composition of the synthesised LCSO powder was further analysed using ICP-MS. Table 3 summarizes the chemical composition of the LCSO powder obtained from the analysis. Based on the data, all the elements of the synthesised LCSO powder can be found except for O as the ICP-MS was unable to detect the O element. With reference to the theoretical mass of the elements in the compound, the percent recovery of Li, Co and Sr was 66.00%, 98.45% and 96.57%, respectively. The low percentage recovery of Li may be due to the high calcination temperature during the synthesis process. This result is in coherence with the XRD results, at 900 °C calcinations, the percentage of Li in LCSO powder is lower than that of LCSO powder calcined at 800 °C, indicating Li loss at high temperatures. Ganas et al. explained that high-temperature treatment is effective to introduce oxygen vacancies in $Li[Ni,Mn]O_4$ cathode material [29]. Partial loss of lithium may lead to the formation of oxygen vacancies in the LCSO cathode. These oxygen vacancies can act as active sites for the ORR, enhancing the catalytic activity of the cathode, thus improving the oxygen surface exchange kinetics at the cathode-electrolyte interface [30].

Table 3. Theoretical mass and actual mass of LCSO powder.

Element	**Theoretical Mass * (mg)**	**Actual Mass * (mg)**
Li	0.63	0.42
Co	3.23	3.18
Sr	3.21	3.10
O	2.93	nd

* The total mass used for the analysis was 10 mg; nd-not detected.

3.1.3. Microstructure Analysis

The cross-sectional FESEM images and the porosity illustration from the surface of the LCSO/YSZ and LCSO/SDC symmetrical cells are shown in Figure 6a(i)–d(i),a(ii)–d(ii), respectively. Based on the cross-sectional images, it can be seen that the application of two layers of LCSO cathode ink resulted in a 17–22 μm film thickness on the surface of the electrolyte. Both YSZ and SDC electrolytes produce a dense and compact layer, which is a desirable structure for SOFC applications. An electrolyte for SOFCs should be dense rather than porous. A dense electrolyte material ensures that the fuel and oxidant gases do not leak through the cell and maintains the separation between the anode and cathode

compartments. It also facilitates efficient ion transport within the electrolyte, allowing for the desired electrochemical reactions to occur at the electrode interfaces.

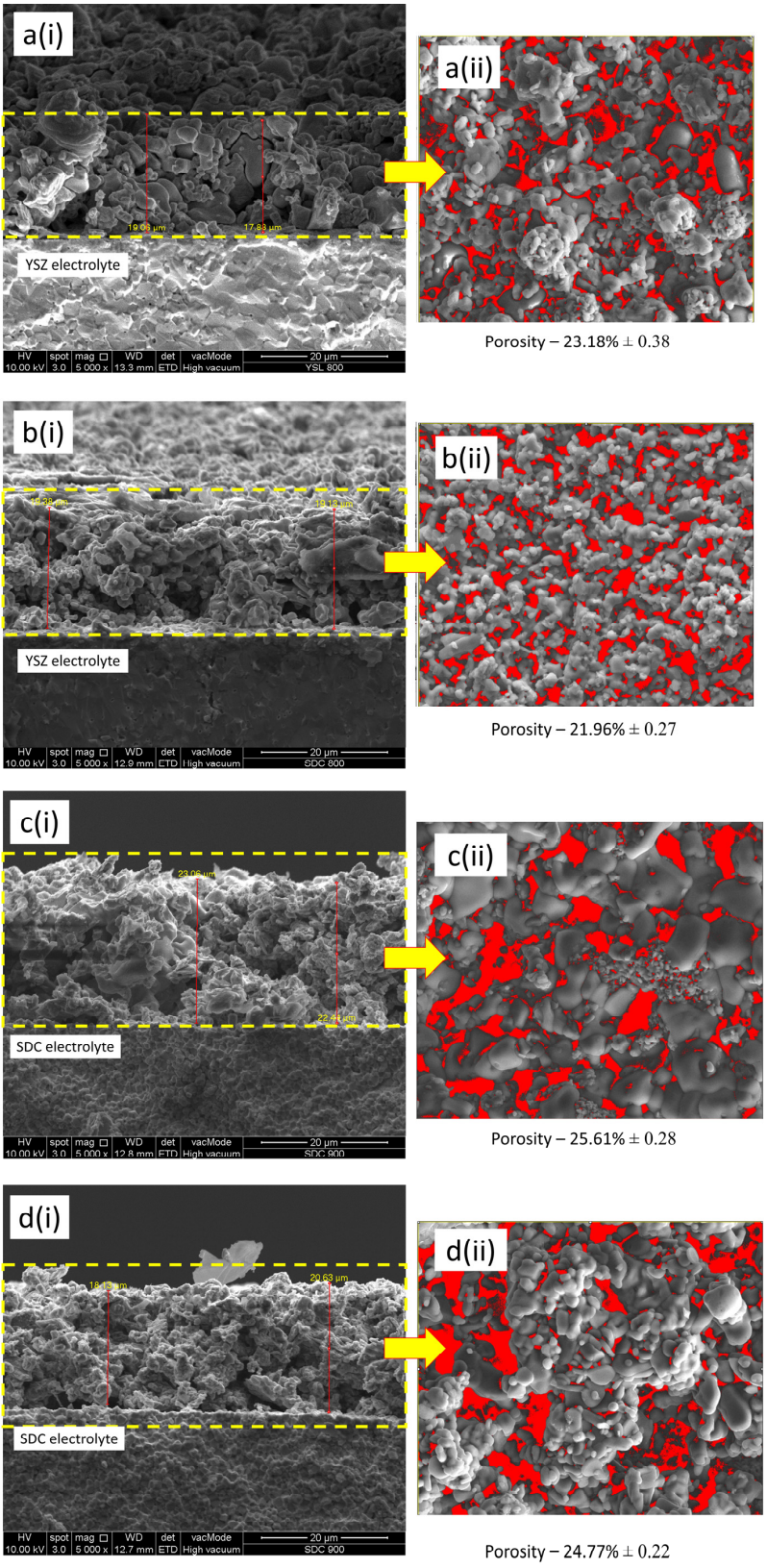


Figure 6. FESEM images for the symmetrical cells of (**a**) 800 °C LCSO/YSZ, (**b**) 900 °C LCSO/YSZ, (**c**) 800 °C LCSO/SDC, and (**d**) 900 °C LCSO/SDC (**i**) Cross-sectional and (**ii**) porosity illustrations of the surface region for the symmetrical cells at 20 µm magnification.

Meanwhile, LCSO cathode with an 800 °C calcination temperature (Figure 6a(ii),c(ii)) produces a more porous structure compared to a 900 °C calcination temperature, as shown in Figure 6b(ii),d(ii). The porosity of the cathode is important for effective gas diffusion and access to the electrochemically active sites. A porous cathode allows for the infiltration of oxygen gas and facilitates the ORR at the cathode-electrolyte interface. The porosity also promotes good contact between the cathode and the electrolyte, ensuring efficient ion transport within the cell. Therefore, a porous LCSO cathode is desired to enhance the performance of the symmetrical cell and enable efficient electrochemical reactions.

Theoretically, the choice of electrolyte material does not directly affect the porosity of the cathode during the formation of a symmetrical cell. The porosity of the cathode is primarily determined by the fabrication method, the specific composition of the cathode material, and the processing parameters, such as the choice of binders, the mixing technique, and the subsequent heat treatment. The choice of electrolyte material primarily affects ionic conductivity, oxygen ion mobility, and chemical compatibility within the cell. However, based on the porosity illustration, the porosity of the LCSO cathode is affected by the difference in the electrolyte as the porosity trend changes when the electrolyte was changed. This phenomenon can be explained based on the compatibility of the thermal expansion coefficient (TEC) of the electrolyte and the LCSO cathode. YSZ has a relatively high TEC, which can lead to a mismatch in thermal expansion with LCSO cathode materials, thus a less porous structure. SDC electrolyte has a lower TEC, producing a more compatible and porous structure.

Further analysis on the surface region of the LCSO cathode calcined at 800 °C shows that the particles formed a layered or spinel crystal structure ranging from 0.3 to 1.1 µm as shown in Figure 7a(iii),c(iii). Figure 7b(iii),d(iii) show that the grain grew and formed more agglomeration after 900 °C of calcination. Furthermore, using a different electrolyte for the symmetrical cell significantly changes the morphological structure of the LCSO cathode. For the YSZ electrolyte in Figure 7a(i),b(i), the LCSO cathode forms a uniform porous structure, while for the SDC electrolyte in Figure 7c(i),d(i), the LCSO cathode fused together and formed larger non-uniform porous structures.

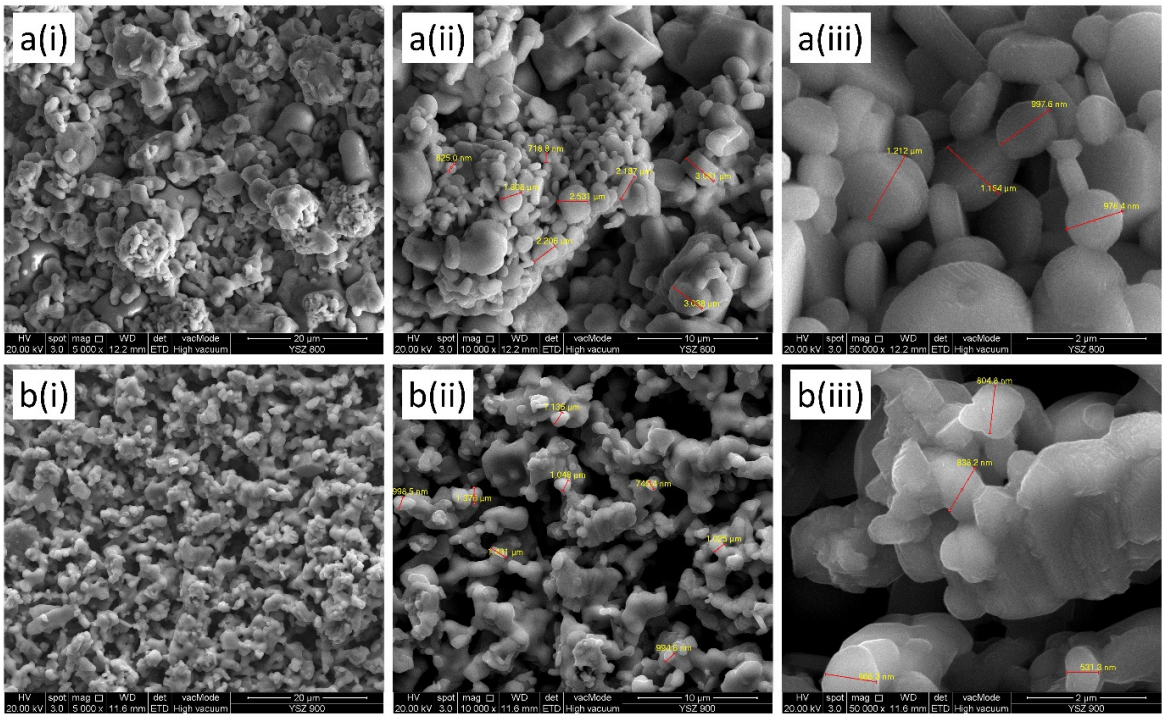


Figure 7. *Cont.*

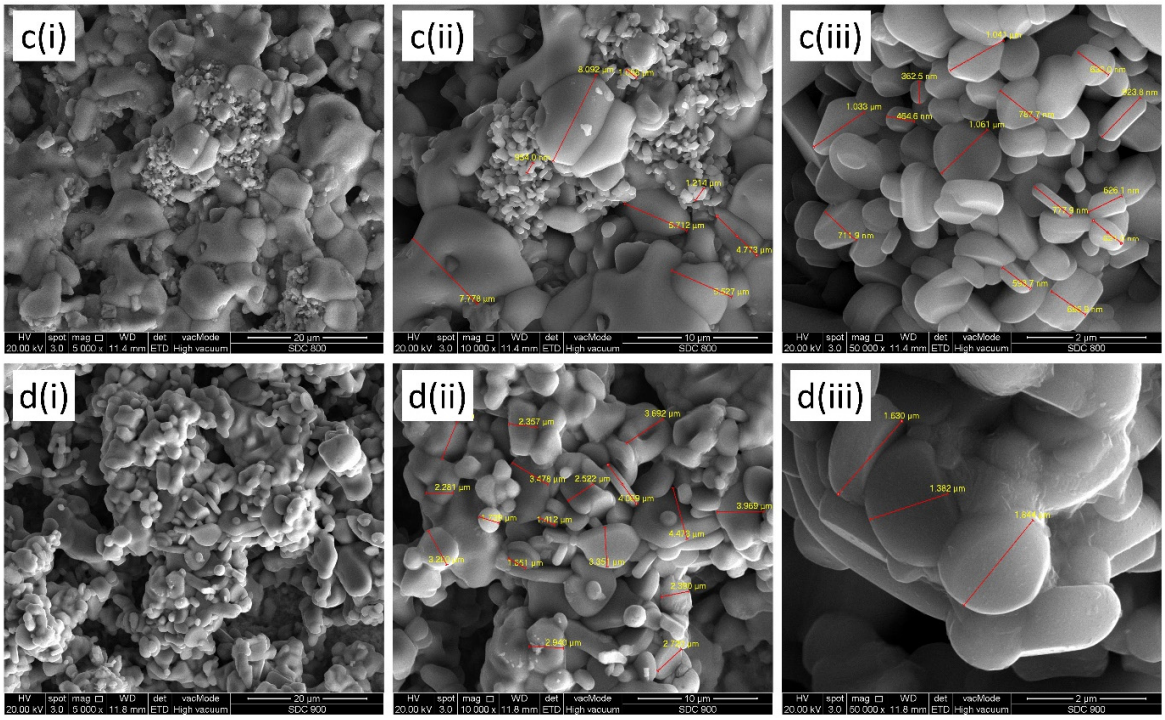


Figure 7. FESEM images of the surface region at different magnifications (**i**) 20 µm, (**ii**) 10 µm, and (**iii**) 2 µm for symmetrical cells (**a**) 800 °C LCSO/YSZ, (**b**) 900 °C LCSO/YSZ, (**c**) 800 °C LCSO/SDC, and (**d**) 900 °C LCSO/SDC.

3.2. Electrochemical Performance of the LCSO Cathode

3.2.1. Conductivity and Activation Energy

The conductivity (σ) of the symmetrical cells acquired in a dry air atmosphere at 500–800 °C was plotted as shown in Figure 8. The conductivity of the symmetrical cells was calculated based on Equation (1).

$$\sigma = \frac{L}{RA} \tag{1}$$

where σ is the conductivity of the cell, L is the length/thickness of the symmetrical cell, R is the average resistance, and A is the area of the active layer of the cathode-electrolyte layer in the symmetrical cell.

Based on the result, all the samples exhibit good conductivity at an 800 °C operating temperature. The conductivity of the symmetrical cells is the highest for SDC electrolytes with LCSO calcined at 800 °C. The conductivity value of the LCSO/SDC symmetrical cell started at 0.001 at 500 °C and rose up to 0.038 at 800 °C. A study conducted by Yousaf et al. [31] explained that the high conductivity of a cathode is able to enhance the mass transport and charge transport mechanism of the cell, simultaneously increasing the ORR catalytic activity of the cell by enabling the fast diffusion and additional vacant sites of O vacancies [31].

Based on the Arrhenius plot in Figure 9, the SDC electrolyte with LCSO calcined at 800 °C has the lowest activation energy. The activation energy in this context refers to the ORR reaction to occur, where oxygen molecules from the air combine with electrons and ions at the cathode to produce oxide ions that then migrate through the electrolyte. A low activation energy of the LCSO cathode promotes faster and more efficient oxygen reduction kinetics. It allows the LCSO cathode to facilitate the ORR at lower operating temperatures, reducing the overall energy requirements and improving the cell's performance.

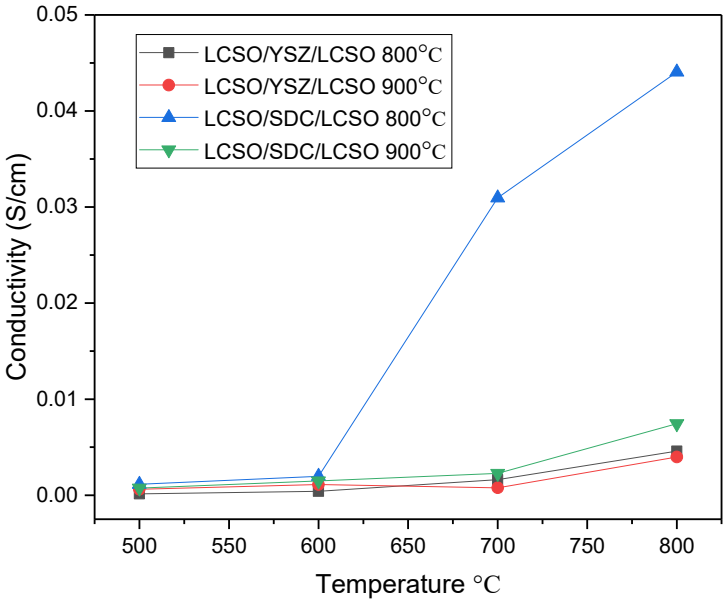


Figure 8. Conductivity of LCSO symmetrical cell calcined at different temperature with different electrolyte.

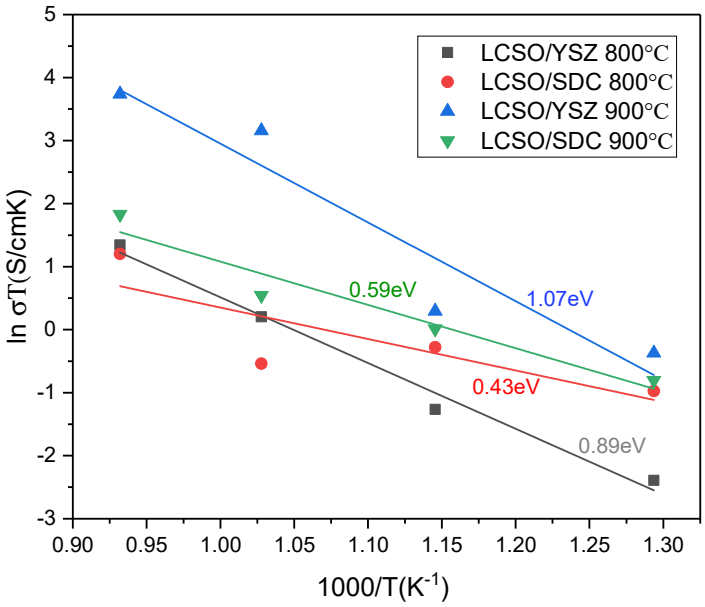


Figure 9. Arrhenius plot of LCSO symmetrical cell with different electrolyte.

3.2.2. Impedance Analysis

The electrochemical studies for all the symmetrical cells were performed in the operating temperature range between 500 and 800 °C in a dry air atmosphere. The area-specific resistance (*ASR*) of the symmetrical cells was calculated based on Equation (2), as shown below.

$$ASR = \frac{R_p}{2} \times A \quad (2)$$

where R_p is the polarisation resistance of the cell and A is the area of the active layer of the cathode-electrolyte layer in the symmetrical cell.

Figures 10 and 11 show the Nyquist plots for the LCSO/YSZ and LCSO/SDC symmetrical cells under dry air, respectively. All the spectra of the symmetrical cells were fitted via the electrical circuit fitting composed of two resistances (R_1 and R_2) and two constant phase

elements (CPE_1 and CPE_2), as shown in the figures. The electrical circuit fitting represents the high- and low-frequency arcs of the spectra. The measured ASR values at different operating temperatures for each symmetrical cell are listed in Table 4.

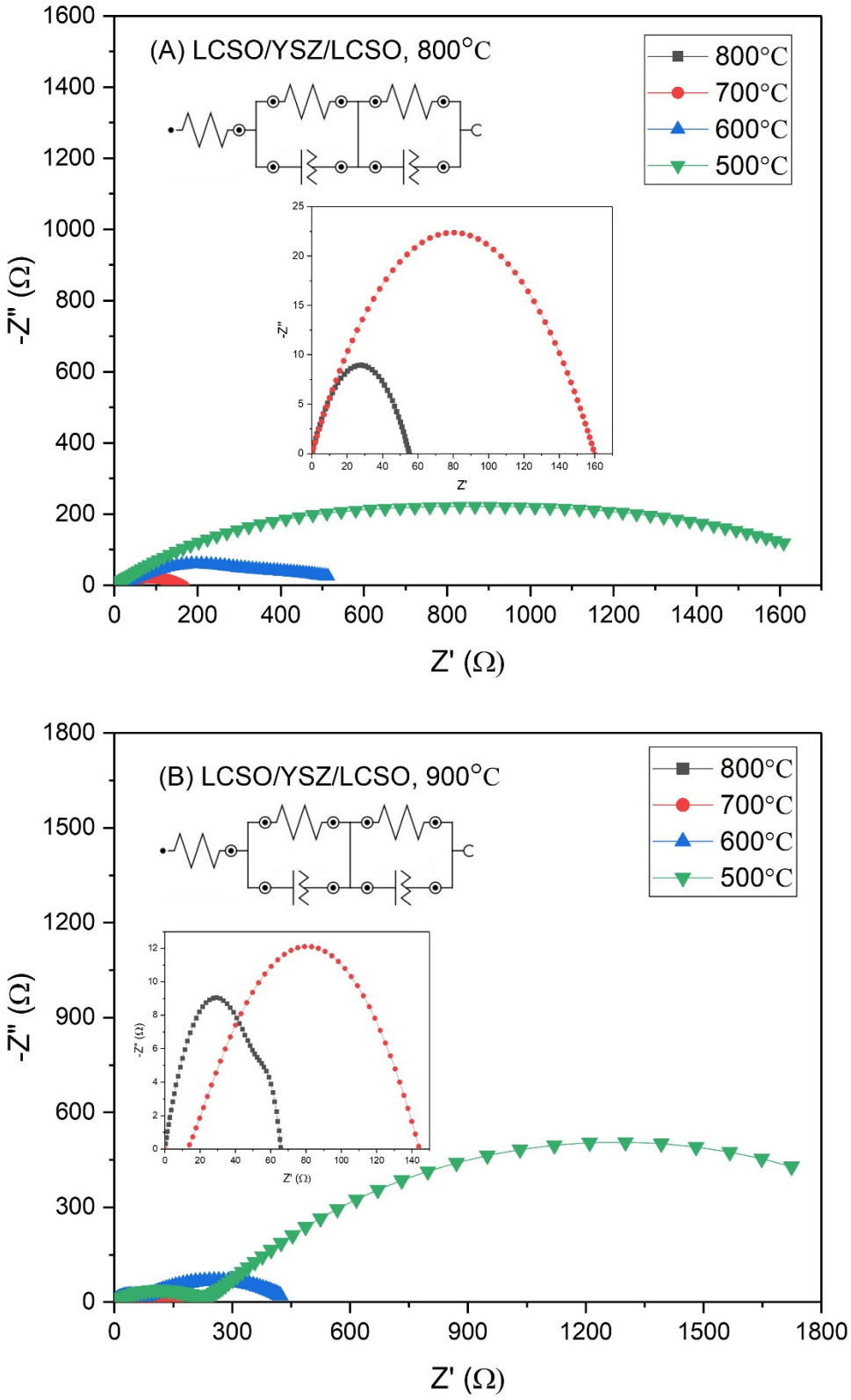


Figure 10. Nyquist plot for LCSO/YSZ/LCSO sample measured at 500–800 °C operating temperatures. The LCSO of the symmetrical cell was calcined at (**A**) 800 °C and (**B**) 900 °C.

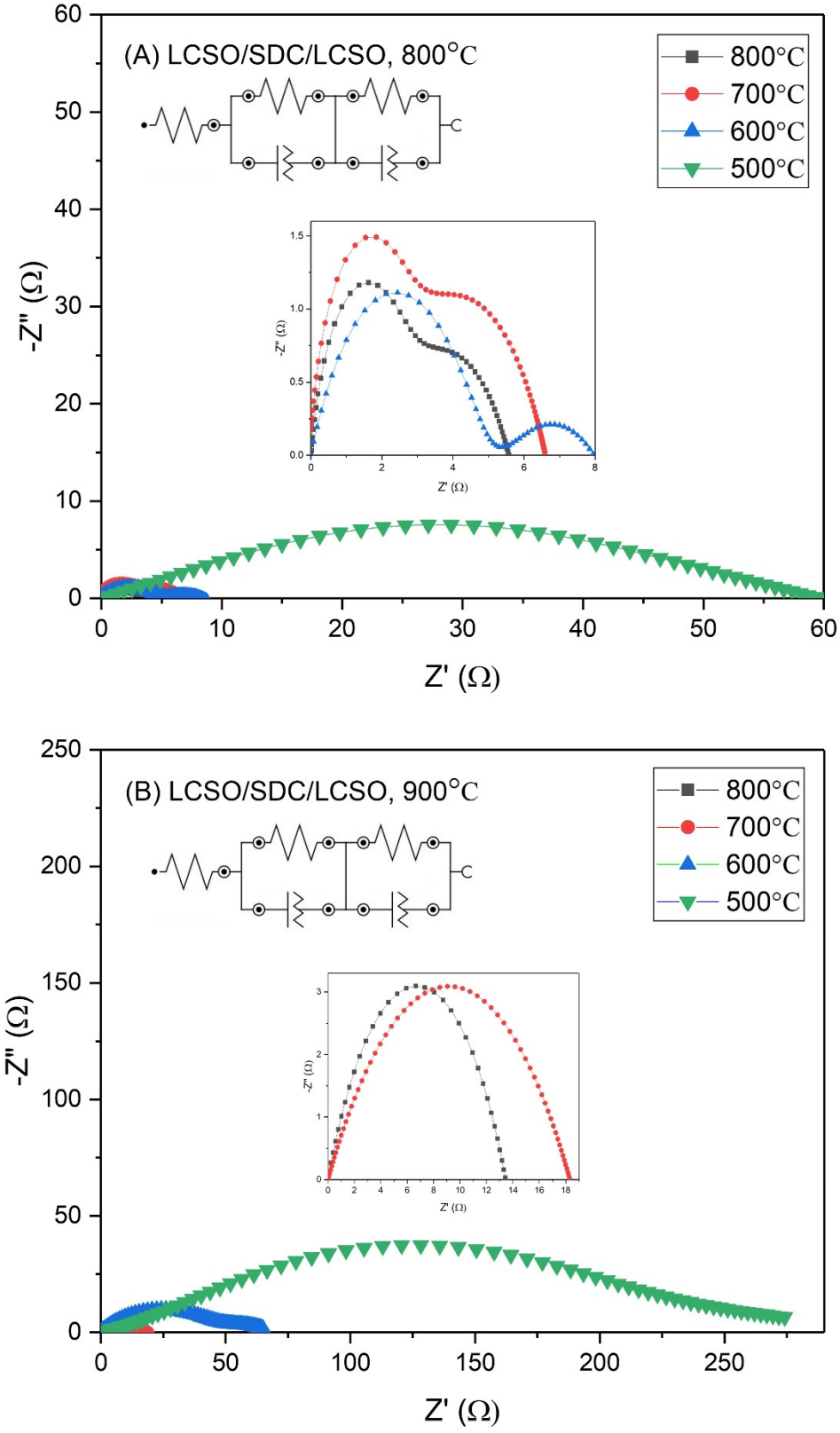


Figure 11. Nyquist plot for LCSO/SDC/LCSO sample measured at 500–800 °C. The LCSO of the symmetrical cell was calcined at (**A**) 800 °C and (**B**) 900 °C.

Table 4. ASR and conductivity values of the symmetrical cells at different operating temperatures.

Symmetrical Cell	Operating Temperature (°C)	ASR (Ω cm^2)	Conductivity ($ohm^{-1}cm^{-1}$)
LCSO/YSZ/LCSO Tc: 800 °C	800	31.70	4.58×10^{-3}
	700	89.80	1.62×10^{-3}
	600	350.500	4.14×10^{-4}
	500	957.00	1.52×10^{-4}
LCSO/YSZ/LCSO Tc: 900 °C	800	36.52	3.97×10^{-3}
	700	94.50	7.68×10^{-4}
	600	130.55	1.11×10^{-3}
	500	231.80	6.26×10^{-4}
LCSO/SDC/LCSO Tc: 800 °C	800	2.89	4.41×10^{-2}
	700	3.34	3.09×10^{-2}
	600	4.69	1.97×10^{-3}
	500	33.2	1.14×10^{-3}
LCSO/SDC/LCSO Tc: 900 °C	800	19.5	7.44×10^{-3}
	700	64	2.27×10^{-3}
	600	194	1.48×10^{-3}
	500	267	7.41×10^{-4}

Tc = Calcined temperature.

Based on the results obtained in Figure 10, it should be noted that the LCSO calcined at 800 °C has a better electrochemical performance with a lower ASR value of 31.70 Ω cm^2 at an 800 °C operating temperature. However, in comparison with the SDC electrolyte in Figure 11, the ASR value of the symmetrical cell shows better performance for both LCSO calcined at 800 °C and 900 °C with 2.89 Ω cm^2 and 19.5 Ω cm^2, respectively. All these results are in agreement with the microstructure analysis of the symmetrical cell in Figures 6 and 7, where the LCSO cathode that was applied to the SDC electrolyte shows more porous structures, thus producing better electrochemical performance. Porous structures of the LCSO cathode increase the overall surface area available for the reaction by facilitating better contact between the electrode, electrolyte, and gas phase, thus providing more active sites for oxygen reduction. This increased surface area leads to a higher density of triple-phase boundary (TPB) sites, promoting more efficient electrochemical reactions.

4. Conclusions

In summary, LCSO cathode calcined at two different temperatures has been successfully applied to the surface of YSZ and SDC electrolytes. LCSO calcined at 800 °C shows a higher crystallinity percentage with more porous structures. In addition, the LCSO cathode calcined at 800 °C has the highest conductivity of 0.038 Scm^{-1} and the lowest activation energy of 0.43 eV. The high conductivity facilitates the movement of electrons and oxygen ions, promoting faster reaction kinetics and reducing the activation energy for the ORR. This enables the LCSO cathode to efficiently facilitate the oxygen reduction process at lower operating temperatures. The porous structure of the LCSO/SDC symmetrical cell also produced better electrochemical performance, with ASR values of 2.89 Ω cm^2 and 19.5 Ω cm^2 for LCSO calcined at 800 °C and 900 °C, respectively. Based on the physicochemical characteristics and electrochemical performance of the symmetrical cell, the SDC electrolyte with LCSO calcined at 800 °C is the promising cathode material for SOFC applications.

Author Contributions: Conceptualization, N.A.B. and S.M.; methodology, S.M.; validation, N.A.B. and S.M.; writing—original draft preparation, S.M.; writing—review and editing, S.M., W.N.A.W.Y. and A.J.A.A.; supervision, N.A.B. and M.R.S.; funding acquisition, N.A.B. All authors have read and agreed to the published version of the manuscript.

Funding: This research was funded by the Universiti Kebangsaan Malaysia under Dana Impak Perdana 2.0 Grant with the grant number of DIP-2022-007 and Dana Pecutan Universiti Kebangsaan Malaysia (PP-SELFUEL-2023).

Data Availability Statement: Not Applicable.

Acknowledgments: The authors gratefully acknowledge the financial support provided for this work by the Universiti Kebangsaan Malaysia for the funding support via the research sponsorship under Dana Impak Perdana 2.0 Grant with the grant number of DIP-2022-007 and Dana Pecutan Universiti Kebangsaan Malaysia (PP-SELFUEL-2023).

Conflicts of Interest: The authors declare no conflict of interest.

References

1. Hussain, S.; Yangping, L. Review of solid oxide fuel cell materials: Cathode, anode, and electrolyte. *Energy Transit.* **2020**, *4*, 113–126. [CrossRef]
2. Kuterbekov, K.A.; Nikonov, A.V.; Bekmyrza, K.Z.; Pavzderin, N.B.; Kabyshev, A.M.; Kubenova, M.M.; Kabdrakhimova, G.D.; Aidarbekov, N. Classification of Solid Oxide Fuel Cells. *Nanomaterials* **2022**, *12*, 1059. [CrossRef] [PubMed]
3. Xu, X. Ceramics in solid oxide fuel cells for energy generation. In *Advances in Ceramic Matrix Composites*, 2nd ed.; Woodhead Publishing: Duxford, UK, 2018; pp. 763–788. [CrossRef]
4. Golkhatmi, S.Z.; Asghar, M.I.; Lund, P.D. A review on solid oxide fuel cell durability: Latest progress, mechanisms, and study tools. *Renew. Sustain. Energy Rev.* **2022**, *161*, 112339. [CrossRef]
5. Mah, J.C.W.; Muchtar, A.; Somalu, M.R.; Ghazali, M.J. Metallic interconnects for solid oxide fuel cell: A review on protective coating and deposition techniques. *Int. J. Hydrogen Energy* **2017**, *42*, 9219–9229. [CrossRef]
6. Wachsman, E.; Ishihara, T.; Kilner, J. Low-temperature solid-oxide fuel cells. *MRS Bull.* **2014**, *39*, 773–779. [CrossRef]
7. Li, Y.; Xu, Z.; Wan, Y.; Zhang, S.; Xia, C. Progress in perovskite anodes for intermediate-temperature solid oxide fuel cells. In *Intermediate Temperature Solid Oxide Fuel Cells*; Elsevier: Amsterdam, The Netherlands, 2020; pp. 195–261. [CrossRef]
8. Shi, H.; Su, C.; Ran, R.; Cao, J.; Shao, Z. Electrolyte materials for intermediate-temperature solid oxide fuel cells. *Prog. Nat. Sci. Mater. Int.* **2020**, *30*, 764–774. [CrossRef]
9. Aziz, A.J.A.; Baharuddin, N.A.; Somalu, M.R.; Muchtar, A. Review of composite cathodes for intermediate-temperature solid oxide fuel cell applications. *Ceram. Int.* **2020**, *46*, 23314–23325. [CrossRef]
10. Yang, G.; Su, C.; Shi, H.; Zhu, Y.; Song, Y.; Zhou, W.; Shao, Z. Toward Reducing the Operation Temperature of Solid Oxide Fuel Cells: Our Past 15 Years of Efforts in Cathode Development. *Energy Fuels* **2020**, *34*, 15169–15194. [CrossRef]
11. Subhashini, P.V.C.K.; Rajesh, K.V.D. Doped BSCF cathode materials for low-temperature solid oxide fuel cell applications-A short review. *Mater. Today Proc.* **2022**, *78*, 520–523. [CrossRef]
12. Ghani, F.; An, K.; Lee, D. Effect of Calcination Temperature on the Physicochemical Properties and Electrochemical Performance of FeVO4 as an Anode for Lithium-Ion Batteries. *Materials* **2023**, *16*, 565. [CrossRef]
13. Jo, H.-G.; Ahn, H.-J. Accelerating the Oxygen Reduction Reaction and Oxygen Evolution Reaction Activities of N and P Co-Doped Porous Activated Carbon for Li-O_2 Batteries. *Catalysts* **2020**, *10*, 1316. [CrossRef]
14. Ren, Y.; Cheng, Y.; Gorte, R.J.; Huang, K. Toward Stabilizing Co_3O_4 Nanoparticles as an Oxygen Reduction Reaction Catalyst for Intermediate-Temperature SOFCs. *J. Electrochem. Soc.* **2017**, *164*, F3001–F3007. [CrossRef]
15. He, S.; Jiang, S.P. Electrode/electrolyte interface and interface reactions of solid oxide cells: Recent development and advances. *Prog. Nat. Sci. Mater. Int.* **2021**, *31*, 341–372. [CrossRef]
16. Zhou, X.; Yang, J.; Wang, R.; Zhang, W.; Yun, S.; Wang, B. Advances in lithium-ion battery materials for ceramic fuel cells. *Energy Mater.* **2022**, *2*, 200041. [CrossRef]
17. Kim, J.H.; Baek, S.-W.; Lee, C.; Park, K.; Bae, J. Performance analysis of cobalt-based cathode materials for solid oxide fuel cell. *Solid State Ion.* **2008**, *179*, 1490–1496. [CrossRef]
18. Hu, X.; Xie, Y.; Wan, Y.; Yang, Y.; Wu, X.; Xia, C. Antimony-doped strontium cobalt oxide as promising cathode for low-temperature solid oxide fuel cell with excellent carbon dioxide tolerance. *Appl. Catal. B Environ.* **2021**, *286*, 119901. [CrossRef]
19. Hardy, J.S.; Coyle, C.A.; Bonnett, J.F.; Templeton, J.W.; Canfield, N.L.; Edwards, D.J.; Mahserejian, S.M.; Ge, L.; Ingram, B.J.; Stevenson, J.W. Evaluation of cation migration in lanthanum strontium cobalt ferrite solid oxide fuel cell cathodes via in-operando X-ray diffraction. *J. Mater. Chem. A* **2018**, *6*, 1787–1801. [CrossRef]
20. Dwivedi, S. Solid oxide fuel cell: Materials for anode, cathode and electrolyte. *Int. J. Hydrogen Energy* **2020**, *45*, 23988–24013. [CrossRef]
21. He, Y.; Chen, G.; Zhang, X.; Zhang, L.; Yang, D.; Asghar, M.I.; Geng, S.; Lund, P.D. Mechanism for Major Improvement in SOFC Electrolyte Conductivity When Using Lithium Compounds as Anode. *ACS Appl. Energy Mater.* **2020**, *3*, 4134–4138. [CrossRef]
22. Yang, Y.; Zhang, Y.; Yan, M. A review on the preparation of thin-film YSZ electrolyte of SOFCs by magnetron sputtering technology. *Sep. Purif. Technol.* **2022**, *298*, 121627. [CrossRef]
23. Jiang, S.P. Solid-State Electrochemistry and Solid Oxide Fuel Cells: Status and Future Prospects. *Electrochem. Energy Rev.* **2022**, *5*, 1–47. [CrossRef]

24. Meng, Y.; Wang, X.; Zhang, W.; Xia, C.; Liu, Y.-N.; Yuan, M.; Zhu, B.; Ji, Y. Novel high ionic conductivity electrolyte membrane based on semiconductor $La_{0.65}Sr_{0.3}Ce_{0.05}Cr_{0.5}Fe_{0.5}O_{3-\delta}$ for low-temperature solid oxide fuel cells. *J. Power Sources* **2019**, *421*, 33–40. [CrossRef]
25. Kilner, J.A.; Burriel, M. Materials for Intermediate-Temperature Solid-Oxide Fuel Cells. *Annu. Rev. Mater. Res.* **2014**, *44*, 365–393. [CrossRef]
26. Yusoff, W.N.A.W.; Norman, N.W.; Samat, A.A.; Somalu, M.R.; Muchtar, A.; Baharuddin, N.A. Performance of $LiCo_{0.6}Zn_{0.4}O_2$ as a potential cathode material candidate for intermediate solid oxide fuel cell application. *IOP Conf. Ser. Earth Environ. Sci.* **2019**, *268*, 012139. [CrossRef]
27. Tahir, N.; Baharuddin, N.; Yusoff, W.; Aziz, A.; Somalu, M.; Muchtar, A. Physical and electrochem-ical characteristics of $LiCo_{0.6}Sr_{0.4}O_2$ cathode ink for intermediate-low temperature solid oxide fuel cell. *Malays. J. Anal. Sci.* **2022**, *26*, 640–651.
28. Yusoff, W.N.A.W.; Tahir, N.N.M.; Baharuddin, N.A.; Somalu, M.R.; Muchtar, A.; Wei, L.J. Effects of roller speed on the structural and electrochemical properties of $LiCo_{0.6}Sr_{0.4}O_2$ cathode for solid oxide fuel cell application. *Sustain. Energy Technol. Assess.* **2023**, *56*, 103096. [CrossRef]
29. Ganas, G.; Kastrinaki, G.; Zarvalis, D.; Karagiannakis, G.; Konstandopoulos, A.; Versaci, D.; Bodoardo, S. Synthesis and characterization of LNMO cathode materials for lithium-ion batteries. *Mater. Today Proc.* **2018**, *5*, 27416–27424. [CrossRef]
30. Tang, Z.-K.; Xue, Y.-F.; Teobaldi, G.; Liu, L.-M. The oxygen vacancy in Li-ion battery cathode materials. *Nanoscale Horiz.* **2020**, *5*, 1453–1466. [CrossRef]
31. Yousaf, M.; Akbar, M.; Shah, M.Y.; Noor, A.; Lu, Y.; Akhtar, M.N.; Mushtaq, N.; Hu, E.; Yan, S.; Zhu, B. Enhanced ORR catalytic activity of rare earth-doped Gd oxide ions in a $CoFe_2O_4$ cathode for low-temperature solid oxide fuel cells (LT-SOFCs). *Ceram. Int.* **2022**, *48*, 28142–28153. [CrossRef]

Disclaimer/Publisher's Note: The statements, opinions and data contained in all publications are solely those of the individual author(s) and contributor(s) and not of MDPI and/or the editor(s). MDPI and/or the editor(s) disclaim responsibility for any injury to people or property resulting from any ideas, methods, instructions or products referred to in the content.